

# Thin-film Solar Cells (TFSC) with Copper Zinc Tin Sulfide (CZTS) Absorber Layer using Electrodeposition Technique



# WPI

A Major Qualifying Project Submitted to the Faculty of  
Worcester Polytechnic Institute

in partial fulfillment of the requirement for the  
Degree in Bachelor of Science

In  
Electrical and Computer Engineering

By:

Matthew Breidenbach

Nicole Candanedo

Abraham Cano Ventura

April 25, 2019

Project Advisor:

Professor Maqsood A. Mughal

## **Abstract**

Photovoltaic (PV) systems are a promising alternative to fossil fuels for meeting the increasing energy demand of society. This project focused on analyzing alternative materials indium (III) sulfide ( $\text{In}_2\text{S}_3$ ) and CZTS as the buffer and absorber layers, respectively. Both layers were deposited using electrodeposition with a three-electrode electrochemical cell. The goals of this project were optimizing the deposition parameters for CZTS and synthesizing an n- $\text{In}_2\text{S}_3$ /p-CZTS PV device to analyze its performance parameters. The results revealed the CZTS films had copper-rich, zinc-poor characteristics, giving inconsistent absorption values. In addition, depositing  $\text{In}_2\text{S}_3$  on top of CZTS on Mo-coated glass proved challenging due to its high deposition temperature.

## **Acknowledgements**

We would like to thank our advisor, Professor Maqsood A. Mughal, for all his guidance, patience, and encouragement throughout the course of this project despite the challenges we faced. Professor Mughal for being so understanding and helpful whenever we had any questions or ran into any problems.

We would like to thank the Chemistry & Biochemistry Department for allowing us to use a fume hood and giving us storage space in Lab 006 in Goddard Hall to perform our experiments.

Thank you to Professor John D. Obayemi for training us on how to use the desktop scanning electron microscope in Olin Hall and lending us four sample holders to immediately begin analyzing our samples. Thank you to Professor Pratab M. Rao for allowing us to use equipment in Higgins Lab 026.

A special thank you to Maryam Masroor Shalami for the many hours she spent helping us prepare and analyze our samples. Lastly, thank you to Professor Drew Brodeur for helping us collect absorption data using the spectrophotometer in Goddard Hall 307.

# Table of Contents

Abstract.....	2
Acknowledgements.....	3
Table of Figures .....	6
List of Tables .....	7
Executive Summary .....	8
1: Introduction.....	10
2: Background.....	12
2.1 Current Thin-film Technologies.....	12
2.2 Power Consumption .....	14
3: Experimental Approach .....	15
3.1 Project Objectives .....	15
3.2 In <sub>2</sub> S <sub>3</sub> Solution .....	16
3.3 CZTS Solution.....	17
3.4 Electrodeposition.....	17
3.4.1 Depositing In <sub>2</sub> S <sub>3</sub> .....	19
3.4.2 Depositing CZTS .....	20
3.5 Post Electrodeposition.....	20
3.5.1 Annealing.....	20
3.5.2 Scanning Electron Microscope (SEM) .....	21
3.5.3 Energy-dispersive spectroscopy (EDS) .....	22
3.5.4 Spectrophotometry.....	22
4: Analysis and Results.....	23
4.1 In <sub>2</sub> S <sub>3</sub> Characterization .....	23
4.1.1 In <sub>2</sub> S <sub>3</sub> SEM Analysis.....	24
4.1.2 EDS Results .....	25
4.1.3 Absorption Data.....	27
4.2 CZTS Characterization.....	27
4.2.1 SEM Analysis .....	28
4.2.2 EDS Results .....	29
4.2.3 Absorption Data.....	31
4.3 Devices .....	32

5: Conclusion .....	33
Appendix A.....	34
Appendix B.....	35
References.....	36

## Table of Figures

<i>Figure 1: NREL Best Research Cell-Efficiencies Chart</i> .....	12
<i>Figure 2: U.S. Energy Information Administration World energy consumption</i> .....	14
<i>Figure 3: Electrodeposition setup (Top View)</i> .....	18
<i>Figure 4: Electrodeposition setup (Front View)</i> .....	18
<i>Figure 5: Three-chamber tube furnace</i> .....	21
<i>Figure 6: Scanning electron microscope (SEM)</i> .....	22
<i>Figure 7: Indium sulfide film on Mo-coated glass substrate</i> .....	24
<i>Figure 8: Indium sulfide on PET flexible substrate</i> .....	24
<i>Figure 9: SEM images of indium sulfide (a) as-deposited (b) 250°C (c) 350°C (d) 450°C</i> .....	25
<i>Figure 10: Indium sulfide absorption graph</i> .....	27
<i>Figure 11: CZTS on Mo-coated glass substrate</i> .....	28
<i>Figure 12: CZTS on PET flexible substrate</i> .....	28
<i>Figure 13: SEM images of CZTS (a) as-deposited (b) 250°C (c) 350°C (d) 450°C</i> .....	29
<i>Figure 14: Data from EDS on CZTS films</i> .....	30
<i>Figure 15: CZTS Absorption Data</i> .....	31
<i>Figure 16: Device film where CZTS and Mo layer fell off when attempting to deposit <math>In_2S_3</math></i> .....	32
<i>Figure 17: Device film with non-uniform morphology</i> .....	32

## List of Tables

<i>Table 1: Chemical composition for In<sub>2</sub>S<sub>3</sub> solution.....</i>	<i>16</i>
<i>Table 2: Chemical composition for CZTS solution.....</i>	<i>17</i>
<i>Table 3: Data from EDS on In<sub>2</sub>S<sub>3</sub> films atomic percentage .....</i>	<i>26</i>
<i>Table 4: Data from EDS on CZTS films atomic percentage.....</i>	<i>30</i>

## Executive Summary

With the consumption of energy increasing and the depletion of fossil fuels, renewables become an increasingly important technology to develop. The United States Energy Information Administration projects there will be a 28% increase in world power consumption by the year 2040 as a result of their International Energy Outlook report conducted in 2017 [1]. Renewable energy sources are the fastest-growing energy source, but fossil fuels still make up about three-quarters of the energy consumption [1]. Further improving our sources of renewable energy has become an important task for researchers. Photovoltaic (PV) systems are a promising alternative to fossil fuels for meeting the energy demand of modern society. Currently, cadmium telluride (CdTe), copper indium gallium selenide (CIGS) and cadmium sulfide (CdS) are the most prominent of components for the buffer and absorber layers used in the fabrication of thin-film PV cells. However, cadmium's toxic nature makes it a dangerous chemical to work with, and the chemicals for CIGS are globally scarce [2]. Viable alternatives for the buffer and absorber layers are indium sulfide ( $\text{In}_2\text{S}_3$ ) as the buffer layer and CZTS as the absorber layer.

The work presented had three main goals: synthesizing  $\text{In}_2\text{S}_3$  and CZTS films, then characterizing and optimizing films, and finally fabricating a photovoltaic (PV) device and analyzing its efficiency. The first goal of synthesizing films was achieved by making solutions for both indium sulfide ( $\text{In}_2\text{S}_3$ ) and CZTS. Then films were deposited using electrodeposition to individually get each type of film on a molybdenum (Mo)-coated glass substrate. A three-electrode electrochemical cell was used with an Ag/AgCl reference electrode, a graphite counter electrode (anode), and a molybdenum (Mo)-coated glass or polyethylene terephthalate (PET) flexible substrate as the working electrode (cathode). The film layer of molybdenum on the substrates are 500 nm in thickness.

Deposition of the indium sulfide films took place at a solution temperature of  $150^\circ\text{C}$  stirring at 300 rotations per minute (RPM) with a current density of  $-0.75 \text{ mA/cm}^2$  for 15 minutes. These deposition values were determined to be the optimal deposition parameters by Mughal *et al* [3]. CZTS films were deposited at room temperature while stirring at 300 RPM, at a voltage of  $-1.05 \text{ V}$  for 45 minutes. Both films were deposited on Mo-coated glass and polyethylene terephthalate (PET) flexible substrates. However, to deposit  $\text{In}_2\text{S}_3$  on the PET substrate the deposition



temperature had to be changed to 120°C and deposited for 18.75 minutes, resulting in an indium-rich  $\text{In}_2\text{S}_3$  film.

Characterization of the films was performed by analyzing various performance parameters such as absorbance, stoichiometry, crystalline structure, topology, optical bandgap, and thickness. The parameters analyzed were absorbance, stoichiometry, topology, and optical bandgap. The CZTS deposition parameters were the primary focus for optimization since limited work is available in the electrodeposition of this film. There are various material deposition parameters that influence the performance of a film. The parameters focused on during this project were temperature, deposition time, and current density. Both films were also annealed at temperatures of 250 °C, 350 °C, and 450 °C with sulfurization and under argon gas to solidify the crystalline structure of the films.

The morphology of the films was analyzed by using a scanning electron microscope (SEM). The indium sulfide films showed a higher crack density than expected. No cracks should have been present after depositing with the optimal deposition parameters, and once annealed, a trend of crack density increasing with annealing temperature was observed. Analyzing CZTS with the SEM showed an increase in grain size with an increase in annealing temperature, which was expected. Performing energy-dispersive spectroscopy (EDS) on the films showed the indium to sulfur ratio getting closer to the ideal value of 1.5 with increasing annealing temperature. However, the EDS results for CZTS showed the films were all copper-rich and zinc-poor, which is the opposite of what was expected.

Future work is required for finding the optimal deposition parameters for CZTS to get as close to the ideal stoichiometric ratio as possible. Deposition of  $\text{In}_2\text{S}_3$  films on CZTS also require more research since the PV devices grown often resulted in the CZTS coming off the film due to the high deposition temperature of  $\text{In}_2\text{S}_3$  films.

# 1: Introduction

Further improving our sources of renewable energy has become an important task for researchers. Photovoltaic (PV) systems are a promising alternative to fossil fuels for meeting the energy demand of modern society. Cadmium telluride (CdTe), copper indium gallium selenide (CIGS) and cadmium sulfide (CdS) are the most prominent materials currently used for the buffer and absorber layers in the fabrication of thin-film PV cells. However, because cadmium is a dangerous and toxic chemical to work with, and the chemicals for CIGS are globally scarce, there is a need for the development of new materials [2]. Viable alternatives for the buffer and absorber layer are indium sulfide ( $\text{In}_2\text{S}_3$ ) and CZTS ( $\text{Cu}_2\text{ZnSnS}_4$ ).

$\text{In}_2\text{S}_3$  is a III-IV compound originating from the II-VI semiconductor, replacing group II metals by group III elements [4]. The desired phase to obtain from the film is  $\beta\text{-In}_2\text{S}_3$  since it has a stable state with a tetragonal structure [5]. In addition,  $\text{In}_2\text{S}_3$  has large photosensitivity and direct bandgap of about 2.0–2.3 eV. It has been studied for its photoconductor and photovoltaic applications, achieving a power conversion efficiency of 16.4% when paired with a CIGS absorber layer [6]. The purpose of the work presented is to analyze the relationship between  $\beta\text{-In}_2\text{S}_3$  and kesterite CZTS as the n-type buffer and p-type absorber layer, respectively, using electrodeposition as the deposition method.

Various methods for depositing thin-film solar cells such as E-beam evaporation, ultrasonic spray pyrolysis, sputtering, photochemical deposition, and electrodeposition have been used when attempting to synthesize  $\text{In}_2\text{S}_3$  and CZTS films. These methods usually fall under two categories, vacuum-based or solution-based deposition. Electrodeposition is a low-cost, environmentally-friendly, and high-material-use-efficiency solution-based deposition method when compared to the other methods [7]. In addition, electrodeposition is an advantageous process for mass-production of the films.

The characteristics making kesterite CZTS a suitable absorber layer for a PV system are its direct bandgap of approximately 1.5 eV, high absorption coefficient of over  $10^4 \text{ cm}^{-1}$ , and earth-abundant components [8]. Lin *et al.* used a sputtering process to deposit CZTS films on Mo/SLG substrates at different various working pressures and obtained an efficiency of 5.2% [9]. An efficiency of approximately 12% was reported by Thimsen *et al.* using atomic layer deposition

[10]. Pawar *et al.* followed a similar process to the one presented in this report. Though they did not report a value for their highest efficiency, they were able to obtain bandgap values within the optimal range for the CZTS thin-film.

Numerical simulations of the heterojunction n-In<sub>2</sub>S<sub>3</sub>/p-CZTS solar cell have resulted in efficiency values of 19.2%, with the buffer and absorber layer being 30 nm and 3 μm, respectively [8]. The goals of the work presented are to synthesize the In<sub>2</sub>S<sub>3</sub> and CZTS films, characterize and optimize them, and fabricate a PV device using electrodeposition on molybdenum (Mo)-coated glass and polyethylene terephthalate (PET) flexible substrate.

## 2: Background

There are various drivers for the development of this project including the toxicity or inefficiency of current materials and the projected increase in power consumption worldwide.

### 2.1 Current Thin-film Technologies

Materials currently used in thin-film solar cells range in efficiency and cost to manufacture. The various technologies available, and their efficiencies, are shown in Figure 1. The chart shown is provided by the National Renewable Energy Laboratory, facilitating the visualization of where thin-film technologies stand when compared to its competitors from various companies, organizations, and research institutions.

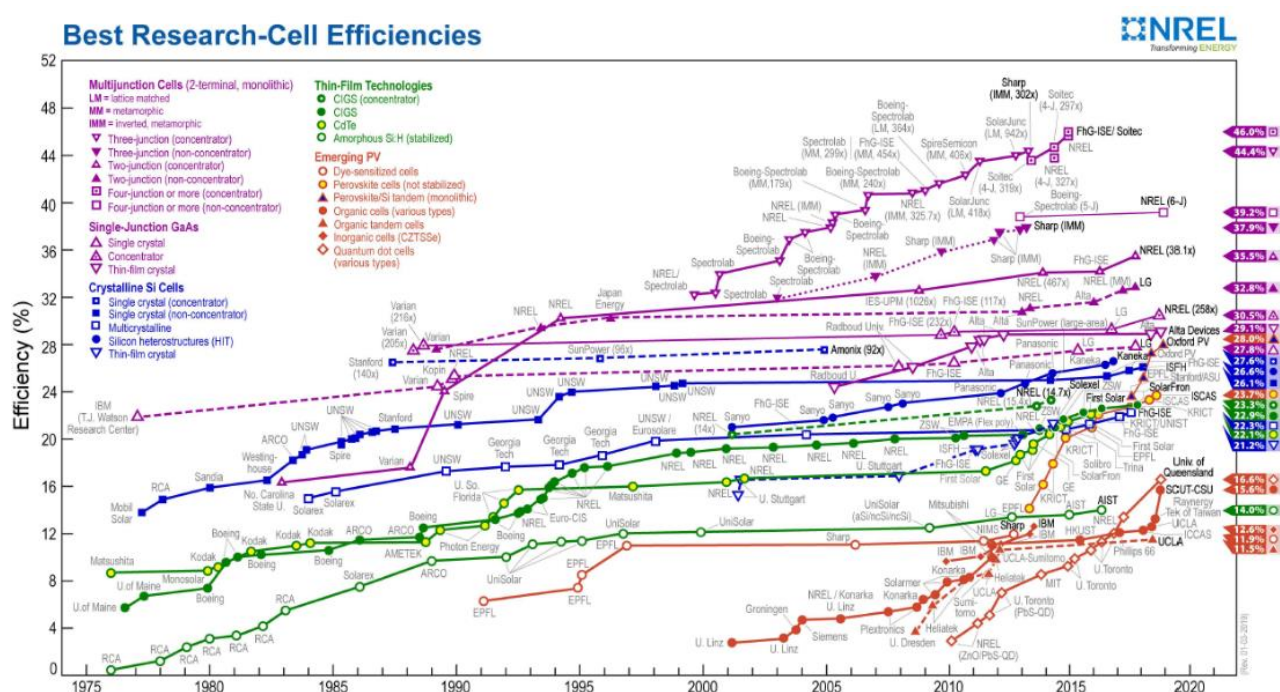


Figure 1: NREL Best Research Cell-Efficiencies Chart

The green lines represent the different materials used in thin-film technologies. Evidently, thin-film technologies fall behind multi-junction cells, which reach efficiencies of 46%. However, multi-junction cells are expensive to manufacture due to expensive materials and a complex manufacturing process [11]. These cells are not currently commercially available, but research is being directed in finding ways to lower the cost of production.

Amorphous silicon (*a-Si*) cells are cheap to manufacture because they use less silicon than other silicon-based cells like crystalline silicon. These low-cost cells have only reached efficiencies as high as 14% in a lab which you can see in Figure 1 above. Due to its low efficiencies, *a-Si* cells are only used in smaller applications such as calculators.

Cadmium telluride (CdTe) is another material used in thin-film technology which has high absorption. It is the second most commonly used worldwide, falling behind crystalline silicon. Manufacturing is quick and inexpensive with average commercial efficiencies of 16.1%, achieved by First Solar in 2015 [12]. Cadmium is used in the synthesis of CdTe solar cells which is a highly toxic material and a known carcinogen. Exposure to it can cause acute pneumonitis, airway obstruction, emphysema and other adverse effects [13]. Tellurium is also toxic as it has been shown to cause kidney, heart, lung and gastrointestinal failure in rats and humans [14]. When disposed of improperly, cadmium from CdTe solar panels can leach into the ground and get into water supplies, which in turn affect humans and wildlife. Although CdTe itself is not toxic, it is still potentially dangerous for the reason of leaching from solar panel disposal.

Copper indium gallium selenide (CIGS) solar cells have reached efficiencies of 12-14% commercially. They have high absorptions, but due to the complexity of producing CIGS cells, it falls behind CdTe in cost [15]. Many different deposition techniques to manufacture these cells have been explored. Current research is aimed at reducing the cost of manufacturing and exploring other metals to use as a back contact in place of molybdenum (Mo).

Gallium arsenide (GaAs) has high absorption but is also expensive to manufacture. Gallium is a byproduct of smelting aluminum and zinc, which is a rare metal, contributing to the expense of manufacturing these films. Arsenic is not rare but is highly poisonous. Like cadmium, arsenic is a known carcinogen and is associated with skin, lung, bladder, kidney and liver cancer [16]. Disposal of GaAs in solid waste landfills comes with risk due to the leaching of arsenic.

Current thin-film materials range in efficiency and some pose serious environmental dangers if disposed incorrectly. For this reason, the development of materials that are environmentally friendly and achieve similar or better efficiencies as materials currently available becomes an important research topic.

## 2.2 Power Consumption

With the consumption of energy increasing and the depletion of fossil fuels, renewables become an increasingly important technology to develop. The United States Energy Information Administration projects there will be a 28% increase in world power consumption by the year 2040 as a result of their International Energy Outlook report conducted in 2017 [1]. Below in Figure 2 is a graph of each energy source and how it is projected to increase over time worldwide. Renewables is the fastest-growing energy source, but fossil fuels still make up about three-quarters of the energy consumption [1]. There is an increasing need to further develop renewables as a result of this increase.

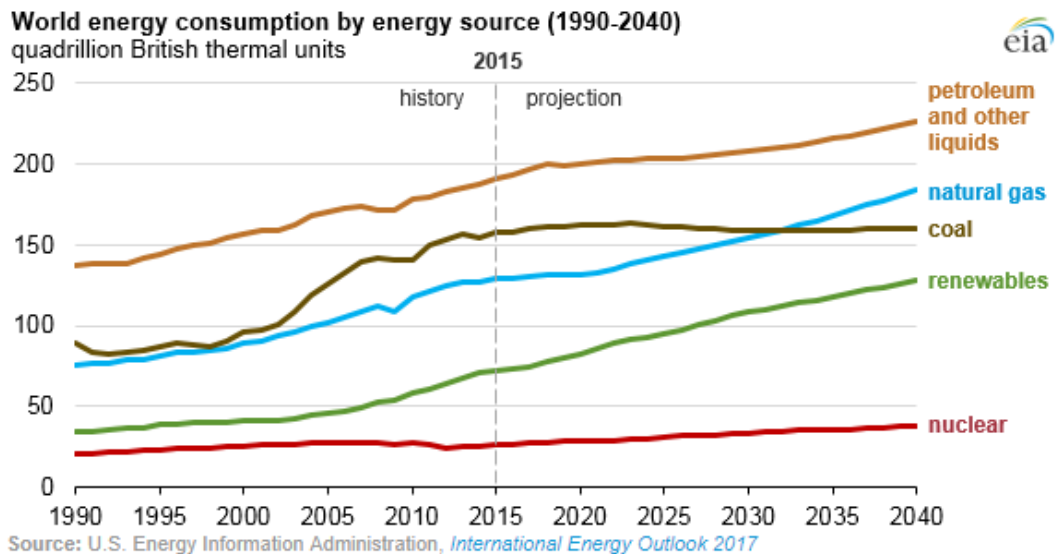


Figure 2: U.S. Energy Information Administration World energy consumption

### **3: Experimental Approach**

This section details the project goals and the plan to achieve them throughout the experimental approach. It also details how the films for the buffer and absorber layers were deposited on Mo-coated glass and PET, as well as how the PV devices were fabricated.

#### **3.1 Project Objectives**

The three main goals for this project were the following:

- 1. Synthesize indium sulfide and CZTS films**
- 2. Characterize and optimize films**
- 3. Fabricate a photovoltaic (PV) device**

The first goal of synthesizing films was achieved by making solutions for both  $\text{In}_2\text{S}_3$  and CZTS. Then, electrodeposition was used to individually deposit each type of film on a 25 mm by 25 mm by 2 mm Mo-coated glass substrate and PET flexible substrate from Tech Instro. The film layer of molybdenum on the substrates were 500 nm in thickness. Once films were deposited, they were characterized.

Characterization of the films can be done by looking at various performance parameters such as absorbance, stoichiometry, crystalline structure, morphology, optical bandgap, and thickness. The parameters analyzed during the allowed time were absorbance, stoichiometry, topology, and optical bandgap. The method for obtaining data on each of these parameters is detailed later in this chapter. Efforts were primarily focused on optimizing the deposition parameters of the CZTS films. There are multiple material deposition parameters that can be changed during the electrodeposition process being voltage, temperature, deposition time, composition of the solution, stir rate, current density, and solvent. Temperature, deposition time, and current density were the main parameters of interest for this project.

Lastly, to achieve our final goal of fabricating a PV device a layer of CZTS was first deposited on the Mo-coated glass.  $\text{In}_2\text{S}_3$  was then deposited on top of the CZTS layer. Ideally, after characterizing CZTS films and optimizing their deposition parameters, using the optimized parameters during electrodeposition would result in a PV device with a non-zero efficiency.

### 3.2 In<sub>2</sub>S<sub>3</sub> Solution

The name of each component needed to make the In<sub>2</sub>S<sub>3</sub> solution, as well as their amount, is shown in Table 1 below in both molarity and grams. The amounts are based on 100mL of ethylene glycol as the solvent. The value in grams for each chemical needed was obtained with the formula in Equation 1 below:

$$\text{molarity (M)} \times \text{liters of solvent (L)} \times \text{molecular weight (g/mol)} = \text{mass (g)} \quad (1)$$

The procedure for making the In<sub>2</sub>S<sub>3</sub> solution is outlined step-by-step in Appendix A.

*Table 1: Chemical composition for In<sub>2</sub>S<sub>3</sub> solution*

<b>Molarity (M)</b>	<b>Chemical</b>	<b>Chemical Formula</b>	<b>Molecular Weight (g/mol)</b>	<b>Amount (g)</b>
0.1	Sulfur	S	32.07	0.32
0.05	Indium chloride	InCl <sub>3</sub>	221.18	1.105
0.1	Sodium chloride	NaCl	58.44	0.58
0.1	Sodium thiosulfate pentahydrate	Na <sub>2</sub> S <sub>2</sub> O <sub>3</sub> * 5H <sub>2</sub> O	248.18	2.481



### 3.3 CZTS Solution

The amount of each chemical needed to make the CZTS solution was also calculated using Equation 1. The values were based on 100 mL of ultrapure water as the solvent and the calculated amounts of each chemical needed is outlined in Table 2.

*Table 2: Chemical composition for CZTS solution*

<b>Molarity (M)</b>	<b>Chemical</b>	<b>Chemical Formula</b>	<b>Molecular Weight (g/mol)</b>	<b>Amount (g)</b>
0.02	Copper (II) sulfate	CuSO <sub>4</sub>	249.69	0.499
0.01	Zinc sulfate	ZnSO <sub>4</sub>	179.47	0.179
0.02	Tin (II) sulfate	SnSO <sub>4</sub>	214.77	0.429
0.02	Sodium thiosulfate pentahydrate	Na <sub>2</sub> S <sub>2</sub> O <sub>3</sub>	248.18	0.496
0.2	Sodium citrate tribasic dihydrate	C <sub>6</sub> H <sub>5</sub> Na <sub>3</sub> O <sub>7</sub> * 2H <sub>2</sub> O	294.10	5.882
0.1	Tartaric acid	C <sub>4</sub> H <sub>6</sub> O <sub>6</sub>	150.09	1.5009

The procedure for making the CZTS solution is outlined step-by-step in Appendix A.

### 3.4 Electrodeposition

Both films were deposited using electrodeposition with a three-electrode electrochemical cell. The electrodeposition setup used in the lab is shown in Figures 3 and 4.

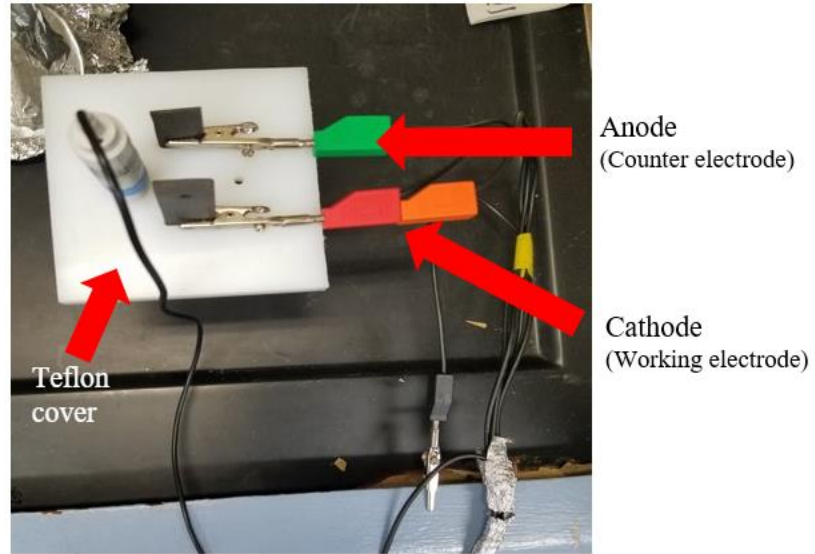


Figure 3: Electrodeposition setup (Top View)

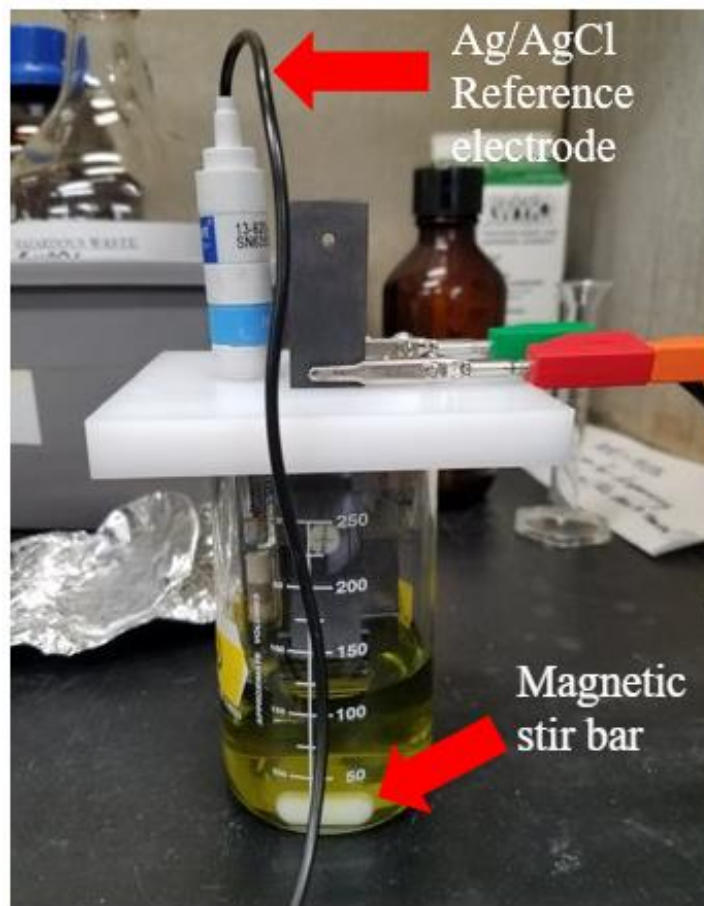


Figure 4: Electrodeposition setup (Front View)

The anode (counter electrode) is a two-inch by two-inch piece of graphite, the cathode (active electrode) is a Mo-coated glass or flexible PET substrate, Ag/AgCl was used as the reference electrode, and the solution was stirred with a magnetic stir bar. All the electrodes are held in place using a polytetrafluoroethylene (Teflon) cover. The cover also keeps the anode and cathode electrodes parallel to each other at a fixed distance to reduce the influence of distance when depositing. A WaveNow Potentiostat from Pine Research Instrumentation was used as an external potentiostat during electrodeposition. This device connects to a laptop via USB and allows the deposition to be in chronopotentiometry or chronoamperometry mode. When set in chronopotentiometry mode the machine provides a constant current and varies the voltage as the film grows. Chronoamperometry provides a constant voltage while varying the current as the film grows.

### 3.4.1 Depositing In<sub>2</sub>S<sub>3</sub>

Deposition of the In<sub>2</sub>S<sub>3</sub> films was done with the WaveNow Potentiostat set to chronopotentiometry mode. Initial In<sub>2</sub>S<sub>3</sub> films were deposited at a current density of -0.75 mA/cm<sup>2</sup> for 15 minutes with a stir rate of 300 rotations per minute (RPM) at 150°C; these are the optimal deposition parameters found by Mughal *et al* [3]. The software used to communicate with the potentiostat was AfterMath, which is also from Pine Research. To use AfterMath the current density needed to be converted to current. Equation 2 has the formula used for converting the current density into current. The surface area used was half the total area of the substrate.

$$\text{Current density} \left( \frac{\text{mA}}{\text{cm}^2} \right) \times \text{Surface area} (\text{cm}^2) = \text{Current} (\text{mA}) \quad (2)$$

Analysis results from the films deposited at -0.75 mA/cm<sup>2</sup> results in films having to be deposited at three new current densities of -0.6 cm<sup>2</sup>, -0.65 cm<sup>2</sup>, and -0.70 cm<sup>2</sup> to better understand the influence of current density on the crack density on the film. These films showed a bright yellow color when deposited on Mo-coated glass.

The optimal deposition parameters had to be changed to deposit In<sub>2</sub>S<sub>3</sub> on the PET substrates. The high temperature of 150°C did not allow for the film to be deposited on the PET, so deposition temperature was changed to 120°C. This temperature was chosen since it is still above the melting point of sulfur; lower temperatures would cause the solution to begin solidifying. Changing the deposition temperature also resulted in the optimal deposition time of 15 minutes to

be increased to 18.75 minutes, making it proportional to the change in temperature. An  $\text{In}_2\text{S}_3$  film as successfully deposited on PET after changing the deposition parameters, however, the film was indium-rich, causing its color to be a dark gray.

### **3.4.2 Depositing CZTS**

Deposition of the CZTS films was done with the WaveNow Potentiostat set to chronoamperometry mode. The films were grown keeping a constant voltage of  $-1.05$  V. The films were deposited without stirring for 45 minutes at room temperature ( $\sim 23^\circ\text{C}$ ). The same Aftermath software was used to deposit the films. Since CZTS is deposited at room temperature, the same parameters were used to deposit a CZTS film on both PET and the Mo-coated glass substrates. CZTS films usually had a dark brown color after being deposited on both types of substrates.

## **3.5 Post Electrodeposition**

### **3.5.1 Annealing**

After the samples were electrodeposited, the films were annealed. Thermal annealing is a process used to solidify the surface topology of materials with temperature and time. The films were annealed using the three-chamber tube furnace shown below in Figure 5. The chambers were set at  $200^\circ\text{C}$ ,  $350^\circ\text{C}$ , and  $500^\circ\text{C}$ . Once the chambers were pre-heated to these temperatures, a temperature probe was used to find out where in the tube furnace the samples needed to be placed for them to be annealed at exactly  $250^\circ\text{C}$ ,  $350^\circ\text{C}$ , and  $450^\circ\text{C}$ . The locations were measured and marked on the hollow glass tube that gets inserted into the furnace. A sample of both  $\text{In}_2\text{S}_3$  and CZTS were placed in each temperature location. Annealing happened for 1 hour under argon gas to avoid oxidation from the open air. The films were also sulfurized to maintain their sulfur since annealing was taking place at a higher temperature than the melting point of sulfur. Steps for setting up the tube furnace can be found in Appendix B.



Figure 5: Three-chamber tube furnace

### 3.5.2 Scanning Electron Microscope (SEM)

An SEM is a type of electron microscope that produces images of a sample by scanning the surface with a focused beam of electrons. The electrons interact with atoms in the sample, producing various signals that contain information about the surface morphology. Once annealed an SEM was used to obtain images of the surface morphology for our samples at magnifications of 500, 1K, 5K, and 10K times. The magnified image of the film allowed for a better way to analyze the films. The SEM used is shown below in Figure 6.



Figure 6: Scanning electron microscope (SEM)

### 3.5.3 Energy-dispersive spectroscopy (EDS)

The machine shown in Figure 6 was also used to perform EDS on the samples. EDS is an analytical technique used to analyze or characterize the stoichiometry of a sample. Its characterization capabilities are due in large part to the fundamental principle that each element has a unique atomic structure allowing a unique set of peaks on its electromagnetic emission spectrum. The EDS results show the percentage of each element on the substrate. The results allow us to compare the percentage of each element to the ideal percentage for analysis of the stoichiometry of the film to determine if it is close to the ideal stoichiometric ratio.

### 3.5.4 Spectrophotometry

Spectrophotometry is a method used to measure how many photons a chemical substance absorbs by measuring the intensity of light as a beam of light passes through the sample. The spectrophotometer used was the Perkins Elmer Lambda 35 UV/VIS Spectrometer shown below in Figure 7.



Figure 7: Spectrophotometer

First a blank sample needs to be scanned in the spectrophotometer to set a baseline reference for the desired sample to be tested. A Mo-coated glass substrate cannot be used a baseline because the molybdenum it is not transparent, therefore the film needs to be grown on a PET substrate.

$$Frequency (Hz) = c / wavelength \quad (3)$$

In the equation above,  $c$  is equal to the speed of light. Once the frequency is found, the bandgap ( $E$ ) is calculated using the Equation 4 below, where  $h$  is plank's constant. These values are then plotted and a trendline is placed to determine the bandgap of our material.

$$E = h \times frequency \quad (4)$$

## 4: Analysis and Results

The performance parameters stoichiometry, optical bandgap, topology, and absorbance for both films were analyzed using data obtained from performing scanning electron microscopy, electron dispersive spectroscopy and spectrophotometry.

### 4.1 In<sub>2</sub>S<sub>3</sub> Characterization

This section will discuss the analysis of the In<sub>2</sub>S<sub>3</sub> films. It will include subsections going into detail about the SEM images, EDS results and the absorption data gathered from

spectrophotometry. Figure 7 below displays  $\text{In}_2\text{S}_3$  on a Mo-coated glass substrate and Figure 8 shows  $\text{In}_2\text{S}_3$  on a PET substrate.

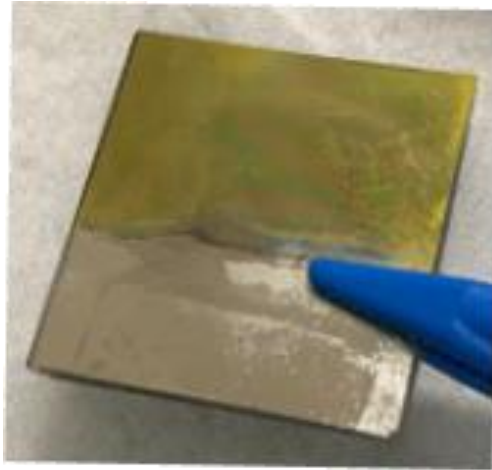


*Figure 7: Indium sulfide film on Mo-coated glass substrate*

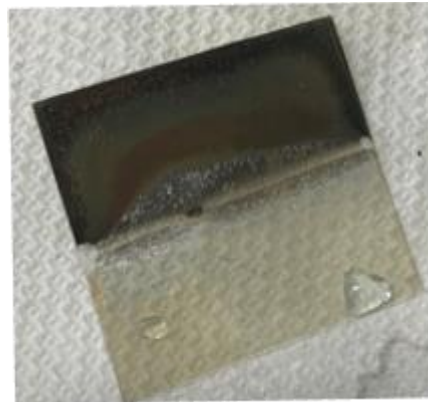


*Figure 8: Indium sulfide on PET flexible substrate*

#### **4.1.1 $\text{In}_2\text{S}_3$ SEM Analysis**

Figure 9 below shows the images obtained on the samples after they were annealed at 250°C, 350°C, and 450°C. As the annealing temperature increased, the crack size and density also increased. The as-deposited samples had more cracks than initially expected and the high crack density was due to a miscalculation of the current. The current was miscalculated by using the wrong area of the film, as a result the films were not grown at the expected current density of - 0.75 mA/cm<sup>2</sup>. The area that was calculated used 1.5 cm as half of the substrate, when the correct



value was 1.25 cm. This miscalculation resulted in a higher current density of  $-0.9 \text{ mA/cm}^2$  leading to more cracks on the surface of the film.

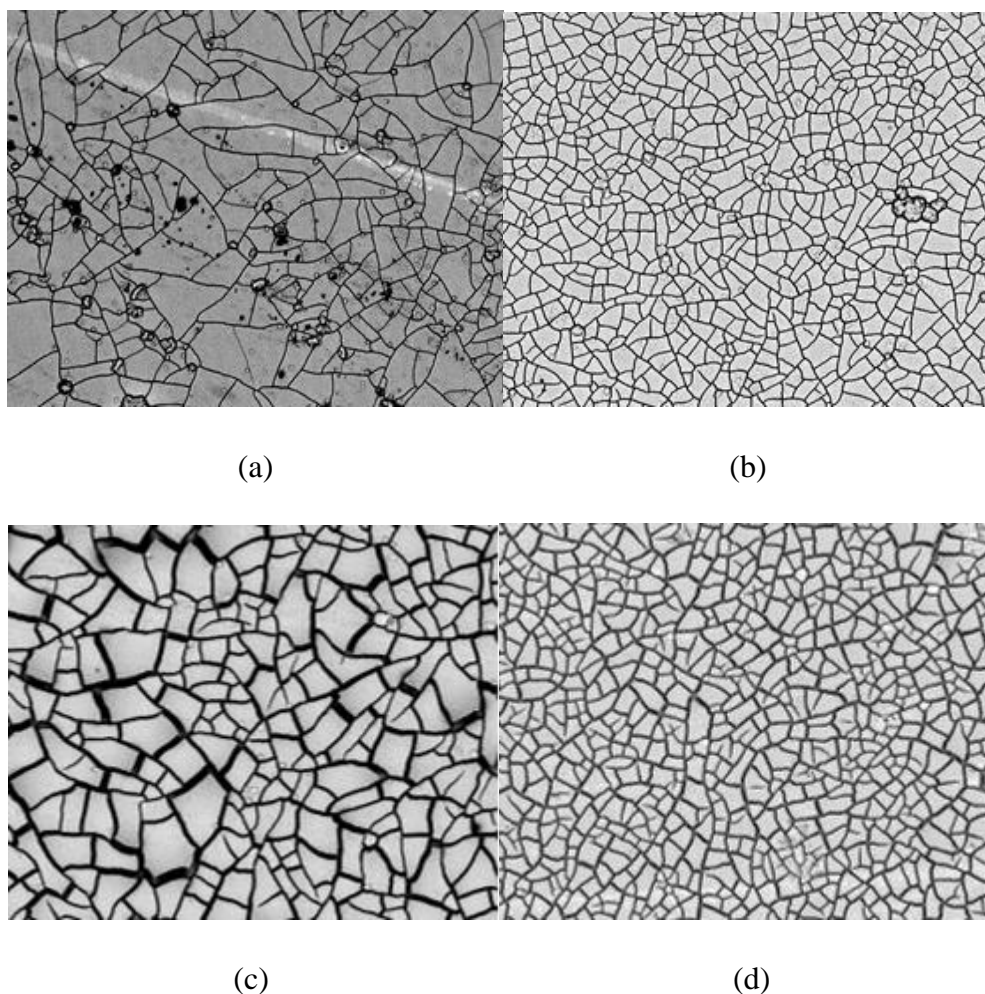


*Figure 9: SEM images of indium sulfide (a) as-deposited (b) 250°C (c) 350°C (d) 450°C*

Following the miscalculation, more films were deposited at a lower current density to lower the number of cracks in the films. Six new films were grown at varying current densities. Two were grown at  $-0.6 \text{ mA/cm}^2$ , two were grown at  $-0.65 \text{ mA/cm}^2$ , and two were grown at  $-0.7 \text{ mA/cm}^2$ .

#### **4.1.2 EDS Results**

When performing the initial EDS analysis of our samples progress was slowed down due to long wait times. Each test on an area of our samples took over 45 minutes and yielded little results. In following weeks, the machine experienced complications and needed maintenance for

a couple weeks after the initial attempts. Once up and running, we ran the analysis again and each attempt took a few minutes to complete, so all the samples were analyzed. We ran the tests on each sample 3 times and the results were averaged. Table 3 below displays the concentrations of Indium and Sulfur in the as-deposited sample as well as the annealed samples.

EDS was performed using the SEM in Higgins Labs on the as-deposited and annealed films to see how annealing affected the stoichiometry of the films. Each spectrum, or analysis, took approximately 6-8 minutes to complete, and more than one spectrum was performed for majority of the films. During the first spectrums performed the EDS took approximately 45 minutes to finish each one, resulting in only one spectrum for CZTS as-deposited,  $\text{In}_2\text{S}_3$  as-deposited and at  $250^\circ\text{C}$ . The EDS was inspected by a technician, reducing the analysis time to the mentioned 6-8 minutes, and three spectrums were performed for the remaining samples. Table 3 below displays the concentrations of indium and sulfur in the as-deposited and annealed films.

*Table 3: Data from EDS on  $\text{In}_2\text{S}_3$  films atomic percentage*

Element	Sulfur (Atm %)	Indium (Atm %)	Ratio S/In
Ideal Atomic %	60	40	1.5
As-deposited	70.2	29.8	0.424
250 °C	57.8	26.6	0.460
350 °C	62.033	37.733	0.608
450 °C	54.633	45.366	0.831

As seen from the results above, the ratio of indium to sulfur is not ideal in the as-deposited and annealed samples. As the annealing temperature increases the sulfur to indium ratio get closer to the ideal value of 1.5 but is still far from the correct ratio by 0.669. This discrepancy in the sulfur to indium ration can be caused by the higher deposition current used due to the calculation error previously stated. The inaccurate ratio is hypothesized to results in inconsistent absorption data.

### 4.1.3 Absorption Data

The  $\text{In}_2\text{S}_3$  film grown on the PET substrate was used to obtain absorption data since the PET substrate is transparent. As previously mentioned, the film could not be grown on the PET using the optimal deposition temperature and time. Due to the non-ideal parameters, the data obtained from spectrophotometry resulted in the graph shown in Figure 10. The graph shows a bandgap of approximately 0.5 eV, substantially lower than the expected value of 2.0-2.3 eV.

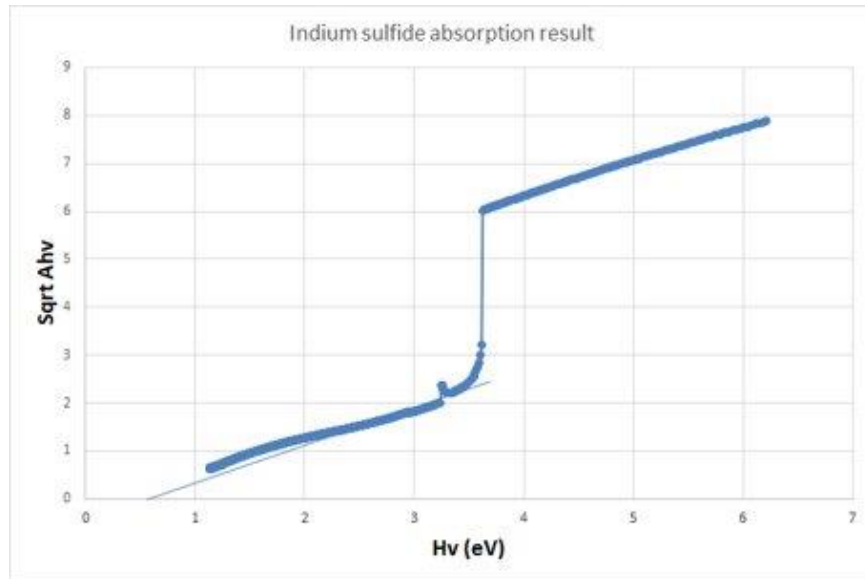
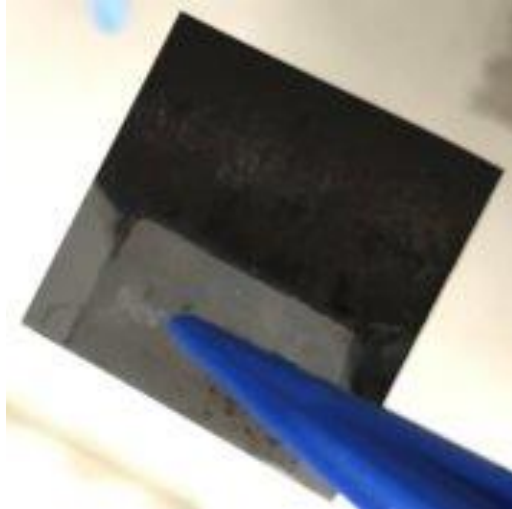


Figure 10: Indium sulfide absorption graph

## 4.2 CZTS Characterization

This section will go into detail of the analysis and characterization of the CZTS films grown over the course of the project. It will describe the SEM images, EDS results and the absorption data gathered from spectrophotometry. Figure 11 below shows the CZTS film deposited on the Mo-coated glass substrate and Figure 12 shows the CZTS film deposited on the PET.



*Figure 11: CZTS on Mo-coated glass substrate*

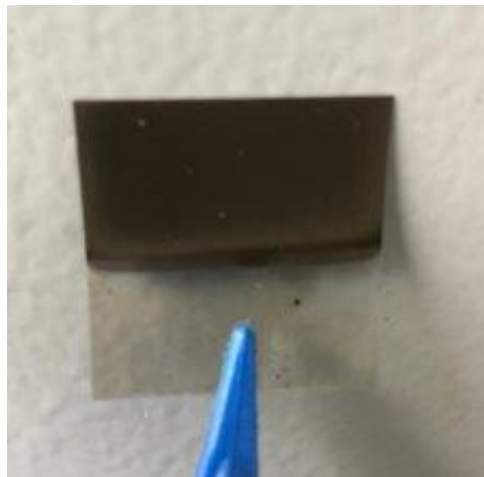


*Figure 12: CZTS on PET flexible substrate*

#### **4.2.1 SEM Analysis**

Images of the CZTS surface as a result of running SEM on the samples can be seen in Figure 13 below.

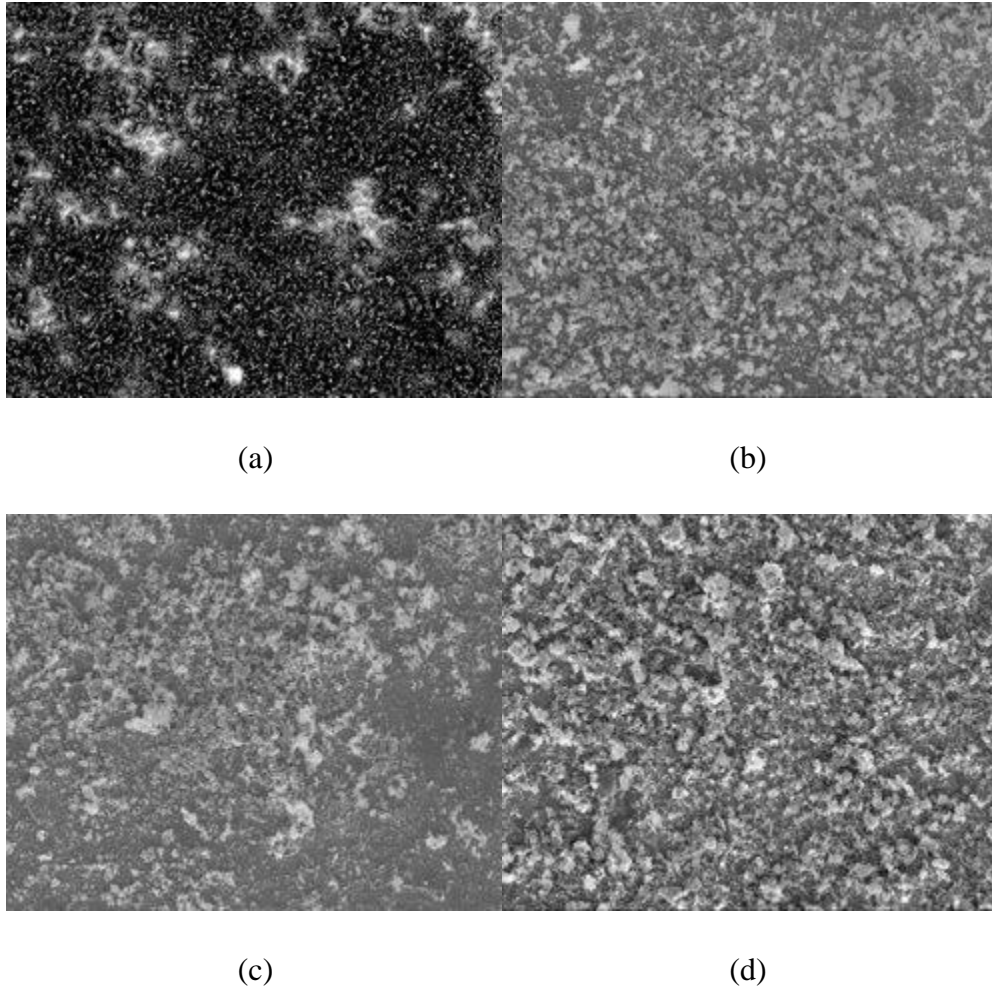


*Figure 13: SEM images of CZTS (a) as-deposited (b) 250°C (c) 350°C (d) 450°C*

Image (a) in Figure 13 above is darker than the rest of the images due to the probe current being set too low. This results in less data points being captured by the microscope of the sample. As the annealing temperature increases the grain size of the films also increases. The purpose of annealing the CZTS films was to solidify the crystalline structure of the film.

#### **4.2.2 EDS Results**

As previously mentioned, initial attempts at performing EDS resulted in longer wait times and little data. The results from the EDS analysis of the CZTS films are shown below visually in Figure 14 and numerically in Table 4.

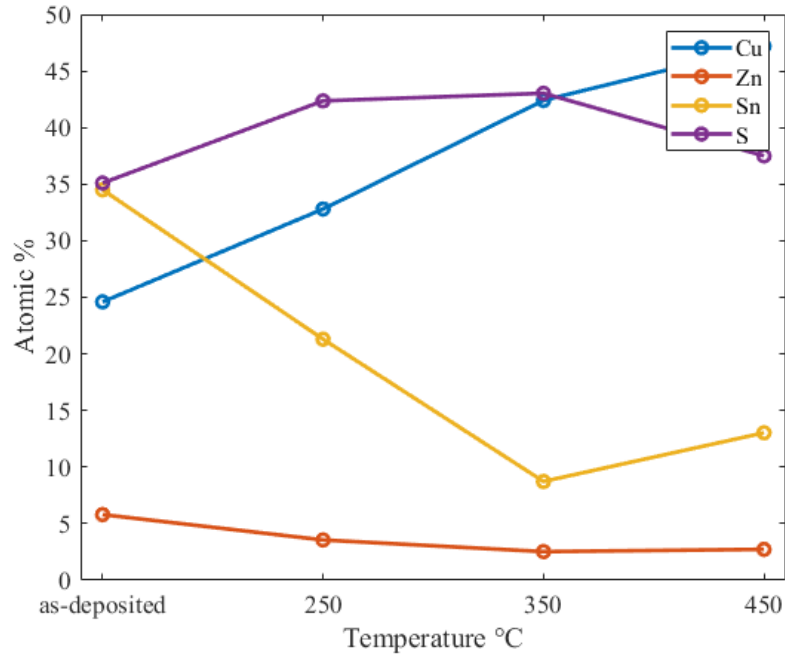


Figure 14: Data from EDS on CZTS films

We can see from the graph that the as-deposited sample contains about the same amount of tin and sulfur. As the samples are annealed, they lose tin and zinc but increase in sulfur and copper. The increase in sulfur is a result of sulfurization.

Numerical values for the atomic percentage of each element for the as-deposited and annealed films are shown in Table 4.

Table 4: Data from EDS on CZTS films atomic percentage

Element	Copper (Atm %)	Zinc (Atm %)	Tin (Atm %)	Sulfur (Atm %)
Ideal Atomic %	25	12.5	12.5	50
As-deposited	24.6	5.8	34.5	35.1
250 °C	32.8	3.56	21.3	42.36
350 °C	42.4	2.53	8.73	43.03
450 °C	47.2	2.73	13.03	37.5

As shown in the results above, the copper was closest to the ideal value in the as-deposited sample. As the annealing temperature increased, the copper concentration went up as well. The

zinc started off low in the as-deposited sample and continued to decrease as the annealing temperature increased. The concentration of tin started off high but decreased as the temperature increased to 450°C where the concentration nearly reached the ideal concentration. Sulfur reacted the opposite way starting with a concentration lower than the ideal and increasing with the annealing temperature increase. At 450°C the sulfur concentration decreased back to a value seen initially in the as-deposited sample.

### 4.2.3 Absorption Data

Contrary to the  $\text{In}_2\text{S}_3$  films, the CZTS parameters were not altered to grow on the PET substrate. Although the parameters used yielded films that were consistent, the results did not match the expected bandgap of approximately 1.5 eV. Figure 15 below shows the graph received from the absorption data.

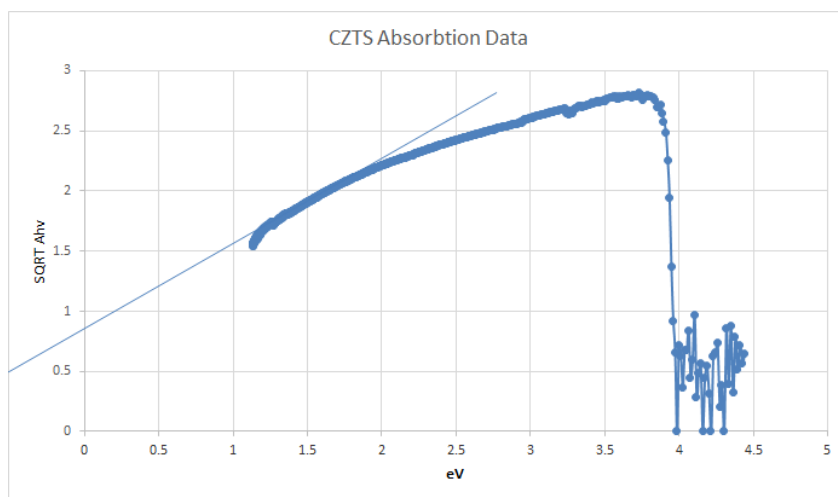


*Figure 15: CZTS Absorption Data*

If the absorption line were to be continued linearly, the line would display a negative bandgap. The negative bandgap is likely due to the copper-rich, zinc-poor film. The non-ideal characteristics resulted in inconsistent results and negative bandgaps. When electrodepositing the samples used to gather the absorption, there wasn't enough potassium chloride and ethylene glycol inside the reference electrode. Moisture might have built up within it making it look like there was enough fluid in it. This also could have been a contributing factor to the incorrect bandgap. When depositing the CZTS films on the PET, the ethylene glycol inside of the reference electrode was approximately three quarters drained from the times it has been used, resulting in poor-quality

films. Adding more ethylene glycol to the reference electrode was difficult due to the fact that exposure to 150°C caused the plastic around the lock of the electrode to melt, sealing the lock in place. The state of the reference electrode is hypothesized to be a cause of the poor absorption characteristics of the CZTS films.

### 4.3 Devices

Substrates that had both  $\text{In}_2\text{S}_3$  and CZTS deposited on them were referred to as devices. First, a CZTS layer was deposited on Mo-coated glass, then the  $\text{In}_2\text{S}_3$  layer was deposited on top of the CZTS layer using the deposition parameters mentioned in sections 3.4.1 and 3.4.2. The deposition of the  $\text{In}_2\text{S}_3$  layer would occasionally result in the CZTS and Mo layer to come off the substrate, as shown in Figure 16.

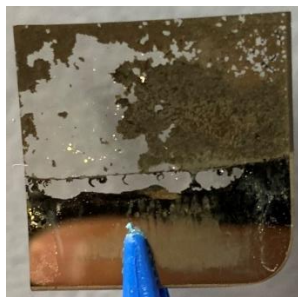


*Figure 16: Device film where CZTS and Mo layer fell off when attempting to deposit  $\text{In}_2\text{S}_3$*

If the deposition of  $\text{In}_2\text{S}_3$  did not cause the CZTS and Mo layers to fall off, another issue would arise, the device layers ended up depositing non-uniformly, as shown in Figure 17.

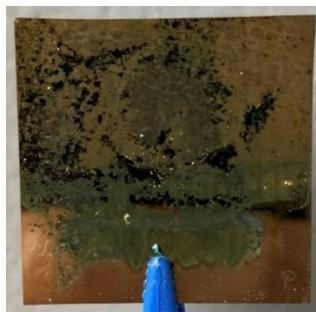


*Figure 17: Device film with non-uniform morphology*

Unfortunately, the equipment necessary for analyzing the performance parameters of the device films for samples where the films did not come off the substrate was not readily available. Therefore, the performance for this heterojunction could not be evaluated during the duration of this project.



## 5: Conclusion

Minimizing the environmental footprint of current PV materials is a field that requires additional development. This project demonstrated that  $\text{In}_2\text{S}_3$  and CZTS are materials that can be electrodeposited on Mo-coated glass substrates and PET for potential use as a PV device. With the challenges faced in accessing equipment essential to analyzing performance parameters for each of the films, work done to optimize the deposition parameters of CZTS films was limited. Lack of access to equipment to analyze characteristics of our PV device resulted in uncharacterized PV cells whose efficiencies remain unknown. Additionally, problems with the lab equipment lead to inconsistencies in the analysis results for the stoichiometry of the films. For future work with this type of project, it would be helpful and beneficial to know in advance that the machines needed would be readily available. The project would move much smoother and faster and more would be accomplished during the short project period.

## Appendix A

### Procedure for making indium sulfide solution and CZTS solution.

#### Indium sulfide:

1. Add 100 mL of ethylene glycol to the beaker
2. Add 0.1 M of sulfur (S)
3. Heat solution to 150°C and stir at 600rpm. Wait for sulfur to fully dissolve (takes approximately 45 mins)
4. Allow solution to cool down to 90°C and add 0.1 M of sodium chloride and 0.5 M of indium chloride with stir rate at 600rpm. Wait about 15 mins for it to dissolve
5. Add 0.1 M of sodium thiosulfate pentahydrate to the solution and wait for it to turn a bright yellow (takes about 15 mins)

The solution usually takes 2-3 hours to complete.

#### CZTS solution:

1. Add 100 mL of ultrapure water to the beaker, leave solution at room temperature and stir at 600rpm
2. Add 0.2 M of copper sulfate and 0.01 M of zinc sulfate. Wait for them to dissolve
3. Add 0.02 M of tin sulfate and 0.02 M of sodium thiosulfate. Wait for them to dissolve
4. Add 0.2 M of sodium citrate and 0.1 M of tartaric acid. Wait for them to dissolve and for the solution to turn a green/brown color (takes about 20 mins)

The solution usually takes 20-30 minutes to complete.

## Appendix B

### Annealing samples

Setting up the tube furnace:

1. Press and hold blue button until you can change the values
2. Assign the program to program 1
3. Set SP1 to 200°C (this is the temperature it will heat up to)
4. Set t1 to 30 mins (0.30)
5. Set SP2 to 200°C (this is the temperature that will be used for the annealing)
6. Set t2 to 1 hour (1.00)
7. Leave SP3 at 0 and have t3 be off (this is the temperature for the furnace to turn off)
8. Press and hold blue button again to save

Repeat steps 1-8 for zone 2 and 3 changing the temperature of SP1 and SP2 to 350 for zone 2 and 500°C for zone 3. Once all zones are set up press the Run button (down arrow) to have the furnace begin working. A red light on the right will turn on once all the zones are running.

Place the 2.5g of Sulfur powder where the temperature in the furnace is 110°C.

### Setting up Argon:

Make sure the meters on the actual argon tube (back left corner of the lab, the tube on the corner) reads 14.6 and the black valve is open. Place the argon feeder in the start of the tube (left side) check to see that it reads around 80. NaOH is used to neutralize the sulfur gas that is caused in the furnace and should be placed at the end of the glass tube (right side). It will be in an Erlenmeyer flask.

A thermometer was used to find the specific zones in the furnace that held the temperature value we needed to use for annealing our samples and for placing the sulfur. The distances measured are:

- 110°C at 2.5cm from the start for sulfur
- 250°C at 40cm from the start
- 350°C at 54.5cm from the end
- 450°C at 45cm from the end

Since the specific zones are hard to find and are only in a small area in the furnace it would be best to set the whole furnace to one temperature and anneal all wanted samples. The procedure mentioned above is due to the necessity for annealing the samples currently available at different temperatures.

## References

- [1] "TODAY IN ENERGY," U.S. Energy Information Administration, 14 September 2017. [Online]. Available: <https://www.eia.gov/todayinenergy/detail.php?id=32912>. [Accessed 21 April 2019].
- [2] B. Unveroglu and G. Zangari, "Towards phase pure kesterite CZTS films via Cu-Zn-Sn electrodeposition followed sulfurization," vol. 219, pp. 664-672, 2016.
- [3] M. A. Mughal, R. Engelken, M. J. Newell, J. Vangilder, S. Thapa, K. Wood, B. R. Carroll and J. B. Johnson, "Morphological and Compositional Analysis of Electrodeposited Indium (III) Sulfide (In<sub>2</sub>S<sub>3</sub>) Films," *Journal of The Electrochemical Society*, vol. 162, no. 7, pp. D265-D269, 2015.
- [4] T. T. John, S. Bini, Y. Kashiwaba, T. Abe, Y. Yasuhiro, C. Sudha Kartha and K. P. Vijayakumar, "Characterization of spray pyrolysed indium sulfide," *Semicond. Sci. Technol.*, p. 491, 2003.
- [5] C. H. Ho, Y. P. Wang, C. H. Chan, Y. S. Hang and C. H. Li, "Temperature-dependent photoconductivity in  $\beta$ -In<sub>2</sub>S<sub>3</sub> single crystals," *Applied Physics*, 2010.
- [6] J. Zhang, H. Wang, X. Yuan, G. Zeng, W. Tu and S. Wang, "Tailored indium sulfide-based materials for solar-energy conversion," *Photochemistry and Photobiology C: Photochemistry Reviews*, vol. 38, pp. 1-26, 2019.
- [7] S. M. Pawar, B. S. Pawar, Moholkar, A. V, D. S. Choi, J. H. Yun and J. H. Moon, "Single step electrosynthesis of Cu<sub>2</sub>ZnSnS<sub>4</sub> (CZTS) thin films for solar cell application," *Electrochimica Acta*, vol. 55, no. 12, pp. 4057-4060, 2010.
- [8] M. A. Mughal, A. Alqudsi, P. M. Rao, M. Masroor, R. Ichwani, L. Zhou and B. Giri, "All-electrodeposited p-Cu<sub>2</sub>ZnSnS<sub>4</sub>/n-In<sub>2</sub>S<sub>3</sub> Heterojunction Formation for Solar Cell Applications," *2018 IEEE 7th World Conference on Photovoltaic Energy Conversion (WCPEC) (A Joint Conference of 45th IEEE PVSC, 28th PVSEC & 34th EU PVSEC)*, pp. 142-147, June 2018.
- [9] Y. P. Lin, Y. F. Chi, T. E. Hsieh, Y. C. Chen and K. P. Huang, "Preparation of Cu<sub>2</sub>ZnSnS<sub>4</sub> (CZTS) sputtering target and its application to the fabrication of CZTS thin-film solar cells," *Journal of Alloys and Compounds*, vol. 654, pp. 498-508, 2016.
- [10] E. Thimsen, S. Riha, S. Baryshev, A. Martinson, J. Elam and M. Pellin, "Atomic Layer Deposition of the Quaternary Chalcogenide Cu<sub>2</sub>ZnSnS<sub>4</sub>," *Chemistry Of Materials*, vol. 24, no. 16, pp. 3188-3196, 2012 .

- [11] "Multijunction III-IV Photovoltaic Research," Energy Efficiency & Renewable Energy, [Online]. Available: <https://www.energy.gov/eere/solar/multijunction-iii-v-photovoltaics-research>. [Accessed 21 April 2019].
- [12] "Cadmium Telluride," Energy Efficiency & Renewable Energy, [Online]. Available: <https://www.energy.gov/eere/solar/cadmium-telluride>. [Accessed 21 April 2019].
- [13] "U.S. National Library of Medicine," [Online]. Available: <https://hazmap.nlm.nih.gov/category-details?id=2&table=copytblagents>. [Accessed 21 April 2019].
- [14] "Evaluation of tellurium toxicity in transformed and non-transformed human colon cells," US National Library of Medicine National Institutes of Health, [Online]. Available: <https://www.ncbi.nlm.nih.gov/pubmed/23068156>. [Accessed 21 April 2019].
- [15] "Copper Indium Gallium Diselenide," Energy Efficiency & Renewable Energy, [Online]. Available: <https://www.energy.gov/eere/solar/copper-indium-gallium-diselenide>. [Accessed 21 April 2019].
- [16] "Arsenic," National Institute of environmental Health Science, [Online]. Available: <https://www.niehs.nih.gov/health/topics/agents/arsenic/index.cfm>. [Accessed 21 April 2019].
- [17] K. Ramasamy, M. A. Malik and P. O'brien, "Routes to copper zinc tin sulfide  $Cu_2ZnSnS_4$  a potential material for solar cells," *Chemical Communications*, vol. 48, no. 46, pp. 5703-5714, 2012.